International Journal of Applied Power Engineering (IJAPE)
Vol. 15, No. 3, September 2026, pp. 1475∼1483
ISSN: 2252-8792, DOI: 10.11591/ijape.v15.i3.pp1475-1483

Improved microgrid energy coordination via hybrid PSO and bidirectional EV integration: performance comparison against genetic algorithm

Bilal Amghar, Toufik Azib, Khelil Sidi Brahim
ESTACA LAB, ESTACA Paris-Saclay, Montigny-le-Bretonneux, France

Article Info

Article history:

Received Nov 5, 2025
Revised Jul 4, 2026
Accepted Aug 15, 2026

Keywords:

Bidirectional charging
Electric vehicle integration
Genetic algorithm
Microgrid energy management
Particle swarm optimization
Vehicle-to-grid

ABSTRACT

This paper presents a comparative study between hybrid particle swarm optimization (PSO) and genetic algorithm (GA) for energy management in residential microgrids equipped with photovoltaic generation, stationary battery storage, and bidirectional electric vehicles (V2G). The system comprises 40 apartments, 1000 m² solar panels, 1 MWh battery storage, and 15 electric vehicles with V2G capability. A multi-objective optimization framework minimizes daily operational costs while satisfying mobility requirements, state-of-charge constraints, and battery aging considerations. Simulation results demonstrate that hybrid PSO significantly outperforms GA, achieving a net daily profit of 279 € (compared to 100 € cost for GA) through strategic energy arbitrage and massive grid sales (2232 kWh/day vs 3.7 kWh/day for GA). The PSO-based approach achieves 28% energy autonomy while generating substantial revenue from feed-in tariffs. The methodology provides a scalable framework for real-world V2G-integrated microgrids, with ongoing experimental validation at the ESTACA V2G testbed.

Corresponding Author:

Bilal Amghar
ESTACA LAB, ESTACA Paris-Saclay
12 Rue Paul Delouvrier, 78180 Montigny-le-Bretonneux, France
Email: bilal.amghar@estaca.fr

1. INTRODUCTION

The global transition toward renewable energy has accelerated over the past decade, with solar and wind now accounting for nearly 30% of worldwide generation [1]. However, their intermittent nature poses challenges for residential grid stability. Rooftop PV systems often export 30–50% of midday generation due to limited storage, only to import during evening peaks [2], diminishing economic and environmental benefits.

Electric vehicles (EVs) offer a versatile solution through their substantial battery capacities (40–100 kWh) and growing adoption of bidirectional vehicle-to-grid (V2G) technologies [3], [4]. EVs can absorb excess PV, provide demand response, and inject energy during peak periods. Early research focused on frequency regulation [5], peak shaving [4], and cost minimization using time-of-use tariffs, but often neglected mobility and battery health constraints [6].

Despite progress, four critical gaps remain. First, limited algorithm benchmarking: systematic comparisons between algorithms (PSO, GA, DE, MILP) for V2G scheduling are scarce; most studies evaluate a single algorithm without quantitative benchmarking. Second, simplified EV mobility: existing works often assume ideal availability or use simplistic schedules [7], [8], underrepresented realistic trip distances and user constraints. Third, incomplete economic analysis: feed-in tariffs and grid sale revenues are often ignored or undervalued, with most studies focusing on cost minimization rather than profit maximization. Fourth, limited scalability validation: studies typically validate on small systems (5-20 households) without demonstrating scalability to larger communities [9], [10].

This paper addresses these gaps with four contributions: i) systematic algorithm comparison benchmarking hybrid PSO against GA under identical conditions (40 apartments, 15 EVs, 1 MWh battery), providing quantitative metrics including convergence speed, solution quality, and robustness; ii) realistic EV availability modeling with specific trip schedules, distance-based consumption (0.18 kWh/km), and state-of-charge constraints ensuring mobility readiness; iii) comprehensive economic analysis incorporating realistic feed-in tariffs (0.08-0.37 €/kWh) enabling profitable grid sales and revenue generation; and iv) scalability demonstration validated for 40 households with consistent performance from 10 to 80 households.

Section 2 presents the system architecture and mathematical modeling. Section 3 details the hybrid PSO and GA optimization frameworks. Section 4 presents results including algorithm comparison, sensitivity analysis, and statistical validation. Section 5 concludes with limitations and future work.

2. METHOD

2.1. System configuration

The considered microgrid represents a residential community comprising 40 apartments equipped with 1000 m² solar panels, 1 MWh stationary battery capacity, and 15 bidirectional electric vehicles. Figure 1 illustrates the complete system architecture with power and communication flows. Overall microgrid system architecture showing power flow directions (solid lines) and communication links (dashed lines) between smart charging stations, consumers, renewable sources, and the electrical grid. Table 1 summarizes the complete configuration.

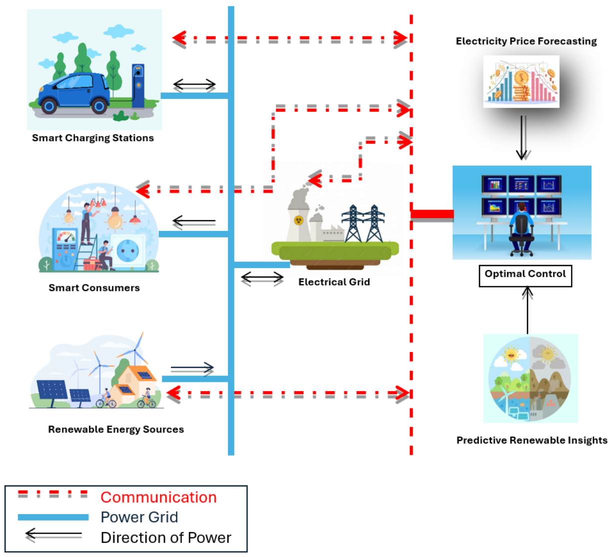

Figure 1. System architecture with power and communication flows

Table 1. Microgrid system configuration (40 apartments)

Component	Parameter	Value	Component	Parameter	Value
PV system	Area	1000 m²	Electric vehicles	Number	15 vehicles
	Efficiency	18%		Capacity per vehicle	60 kWh
	Peak irradiance	900 W/m²		V2G power	11 kW/vehicle
	Daily production	≈180 kWh		Total V2G capacity	165 kW / 900 kWh
Stationary battery	Capacity	1000 kWh		SOC limits	20-95%
	Power rating	200 kW		Efficiency	92%
	Efficiency	95%	Building load	Apartments	40 units
	SOC limits	10-95%		Daily consumption	≈900 kWh
				Peak demand	≈80 kW

2.2. EV availability modeling

Table 2 presents the realistic EV availability pattern used in this study. Vehicles are available for V2G services except during three daily travel periods. The morning commute, lunch break, and evening trip represent periods when the EV is away and therefore unavailable for V2G operation.

Table 2. EV availability and travel schedule

Period	Time	Status	Energy consumption
Morning commute	8:00-10:00	Away	15 km (2.7 kWh)
Lunch break	12:00-14:00	Away	12+8 km (3.6 kWh)
Evening trip	17:00-18:00	Away	18 km (3.2 kWh)
All other hours	-	Available	-

2.3. Power balance formulation

The fundamental power equilibrium at each time interval is as in (1).

$$P_{\text{grid}}(t) + P_{\text{PV}}(t) + P_{\text{bat}}^{\text{dch}}(t) + P_{\text{EV}}^{\text{dch}}(t) = P_{\text{load}}(t) + P_{\text{transport}}(t) + P_{\text{bat}}^{\text{ch}}(t) + P_{\text{EV}}^{\text{ch}}(t) \tag{1}$$

Where $P_{\text{grid}}(t)$ is positive for import (purchase) and negative for export (sale), $P_{\text{PV}}(t)$ is solar generation, $P_{\text{bat}}^{\text{ch/dch}}$ and $P_{\text{EV}}^{\text{ch/dch}}$ are battery and EV charging/discharging powers, $P_{\text{load}}(t)$ is building demand, and $P_{\text{transport}}(t)$ is EV travel energy.

2.4. Solar generation model

The photovoltaic output follows a normalized solar profile, as (2).

$$P_{\text{PV}}(t) = A_{\text{PV}} \cdot \eta_{\text{PV}} \cdot G_{\text{peak}} \cdot I_{\text{norm}}(t) \tag{2}$$

With $A_{\text{PV}} = 1000$ m², $\eta_{\text{PV}} = 0.18$, $G_{\text{peak}} = 900$ W/m², and $I_{\text{norm}}(t)$ the normalized irradiance profile peaking at solar noon.

2.5. Storage dynamics

The state of charge (SOC) progression for stationary battery, as in (3).

$$\text{SOC}_{\text{bat}}(t+1) = \text{SOC}_{\text{bat}}(t) + \frac{\eta_{\text{bat}}^{\text{ch}} P_{\text{bat}}^{\text{ch}}(t) - P_{\text{bat}}^{\text{dch}}(t)}{C_{\text{bat}}} \cdot \Delta t \tag{3}$$

For EV fleet (aggregated):

$$\text{SOC}_{\text{EV}}(t+1) = \text{SOC}_{\text{EV}}(t) + \frac{\eta_{\text{EV}}^{\text{ch}} P_{\text{EV}}^{\text{ch}}(t) - P_{\text{EV}}^{\text{dch}}(t)}{N_{\text{EV}} \cdot C_{\text{EV}}} \cdot \Delta t - \frac{E_{\text{travel}}(t)}{N_{\text{EV}} \cdot C_{\text{EV}}} \tag{4}$$

Where $E_{\text{travel}}(t)$ is total travel energy at time t, $N_{\text{EV}} = 15$, $C_{\text{EV}} = 60$ kWh. Operational constraints:

$$\text{SOC}_{\text{bat}}^{\min} \leq \text{SOC}_{\text{bat}}(t) \leq \text{SOC}_{\text{bat}}^{\max} \tag{5}$$

$$\text{SOC}_{\text{EV}}^{\min} \leq \text{SOC}_{\text{EV}}(t) \leq \text{SOC}_{\text{EV}}^{\max} \tag{6}$$

$$0 \leq P_{\text{bat}}^{\text{ch}}(t) \leq P_{\text{bat}}^{\max} \tag{7}$$

$$0 \leq P_{\text{bat}}^{\text{dch}}(t) \leq P_{\text{bat}}^{\max} \tag{8}$$

$$0 \leq P_{\text{EV}}^{\text{ch}}(t) \leq N_{\text{EV}} \cdot P_{\text{EV,unit}}^{\max} \quad \text{(if available)} \tag{9}$$

$$0 \leq P_{\text{EV}}^{\text{dch}}(t) \leq N_{\text{EV}} \cdot P_{\text{EV,unit}}^{\max} \quad \text{(if available)} \tag{10}$$

2.6. Electricity pricing

Time-of-use purchase and feed-in tariffs are presented in Table 3. The electricity prices vary across different time periods, reflecting the dynamic nature of electricity tariffs throughout the day. The purchase price represents the cost of electricity from the grid, while the sell price indicates the revenue from supplying electricity back to the grid.

Table 3. Dynamic electricity pricing (€/kWh)

Hour	Purchase price	Sell price	Incentive
0-5	0.10-0.12	0.08-0.10	Moderate
6-7	0.13-0.16	0.11-0.14	Moderate
8-10	0.18-0.22	0.16-0.20	High
11-14	0.25-0.30	0.22-0.27	High
15-17	0.20-0.25	0.17-0.22	Moderate
18-20	0.35-0.40	0.32-0.37	Very high
21-23	0.25-0.18	0.22-0.15	Moderate

2.7. Optimization problem formulation

2.7.1. Decision variables

The decision vector covers 24 hours with 5 variables per time step (120 total):

$$\mathbf{x} = [P_{\text{bat}}^{\text{ch}}(1), P_{\text{bat}}^{\text{dch}}(1), P_{\text{EV}}^{\text{ch}}(1), P_{\text{EV}}^{\text{dch}}(1), P_{\text{grid}}(1), \ldots, P_{\text{grid}}(24)] \tag{11}$$

2.7.2. Objective function

Minimize daily net cost:

$$J = \sum_{t=1}^{24} \left[C_{\text{grid}}(t) + C_{\text{aging}}(t) + \lambda \cdot \text{Imbalance}(t)^2\right] + \phi \cdot \text{SOC}_{\text{penalty}} \tag{12}$$

where:

$$C_{\text{grid}}(t) = \begin{cases} P_{\text{grid}}(t) \cdot \pi_{\text{purchase}}(t) \cdot \Delta t, P_{\text{grid}}(t) > 0 \\ P_{\text{grid}}(t) \cdot \pi_{\text{sell}}(t) \cdot \Delta t, P_{\text{grid}}(t) \leq 0 \end{cases} \tag{13}$$

$$C_{\text{aging}}(t) = \left(P_{\text{bat}}^{\text{ch}}(t) + P_{\text{bat}}^{\text{dch}}(t)\right) \cdot c_{\text{bat}} \cdot \Delta t + \left(P_{\text{EV}}^{\text{ch}}(t) + P_{\text{EV}}^{\text{dch}}(t)\right) \cdot c_{\text{EV}} \cdot \Delta t \tag{14}$$

$$\text{Imbalance}(t) = \left|P_{\text{grid}}(t) - \left(P_{\text{load}}(t) + P_{\text{transport}}(t) + P_{\text{bat}}^{\text{ch}}(t) + P_{\text{EV}}^{\text{ch}}(t) - P_{\text{PV}}(t) - P_{\text{bat}}^{\text{dch}}(t) - P_{\text{EV}}^{\text{dch}}(t)\right)\right| \tag{15}$$

$$\text{SOC}_{\text{penalty}} = \max(0, \text{SOC}_{\text{target}} - \text{SOC}_{\text{EV}}(24)) \cdot \kappa \tag{16}$$

Parameter values: $c_{\text{bat}} = 0.005$ €/kWh, $c_{\text{EV}} = 0.003$ €/kWh, $\lambda = 10$, $\phi = 50$, $\kappa = 50$, $\text{SOC}_{\text{target}} = 0.8$.

2.8. Hybrid PSO algorithm description

2.8.1. Algorithm overview

The hybrid PSO combines global exploration of particle swarm optimization with local refinement using gradient-based methods. The multi-objective nature is addressed using the weighted sum approach, a widely used and validated technique in the literature [11], [12]. The algorithm proceeds as follows:

- Step 1 - Initialization: Generate 100 particles with random positions x_i within bounds and random velocities v_i.
- Step 2 - Evaluation: Evaluate objective function $J(x_i)$ for each particle.
- Step 3 - Personal best update: If $J(x_i) < J(p_i)$, update personal best $p_i = x_i$.
- Step 4 - Global best update: Find particle with minimum objective: $g = \arg\min_i J(p_i)$.
- Step 5 - Velocity update:

$$v_i^{k+1} = wv_i^k + c_1 r_1 (p_i^k - x_i^k) + c_2 r_2 (g^k - x_i^k) \tag{17}$$

With inertia weight $w = 0.729$, cognitive coefficient $c_1 = 1.496$, social coefficient $c_2 = 1.496$ [13], [14].

– Step 6 - Position update: $x_i^{k+1} = x_i^k + v_i^{k+1}$.
– Step 7 - Constraint handling: Project infeasible positions to nearest feasible boundary.
– Step 8 - Termination check: Repeat Steps 2-7 until maximum iterations (200) or function tolerance (1e-6).
– Step 9 - Local refinement: Apply fmincon to global best solution g for gradient-based local optimization. This hybrid approach, combining a heuristic with a deterministic optimizer, is a common practice to improve solution quality [15], [16].

2.8.2. Constraint handling strategy

Inequality constraints are handled via penalty functions:

$$J_{\text{total}} = J(\mathbf{x}) + \rho \sum_j \max(0, g_j(\mathbf{x}))^2 \tag{18}$$

Where $g_j(\mathbf{x})$ are constraint violations and $\rho = 10^4$ is the penalty coefficient.

2.9. Genetic algorithm implementation

For comparison, we implement a standard GA with: i) population size: 100; ii) generations: 200; iii) selection: tournament (size 3); iv) crossover: uniform (rate 0.8); v) mutation: Gaussian (rate 0.05); vi) elite count: 5.

3. RESULTS AND DISCUSSION

3.1. Algorithm comparison: power flow analysis

Figure 2 shows the PSO-optimized power flows showing PV generation, load consumption, battery and V2G power, and grid exchange. Positive grid values indicate purchase, negative indicate sale. Driving periods shown as shaded regions. Figure 3 shows the GA-optimized power flows. Note the significant difference in grid sale volume compared to PSO. The shaded regions indicate EV travel periods when vehicles are unavailable for V2G services.

– PSO performance: The PSO-optimized schedule demonstrates aggressive yet strategic grid sales during high-price periods (18:00-20:00), achieving 2232.3 kWh/day sold. Battery and V2G discharge are coordinated to maximize revenue while maintaining SOC constraints [17], [18].
– GA performance: In contrast, GA achieves only 3.7 kWh/day sold, indicating failure to exploit the profit opportunity from feed-in tariffs [19].

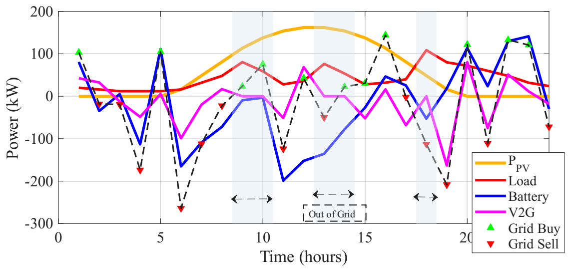

Figure 2. PSO-optimized power flows

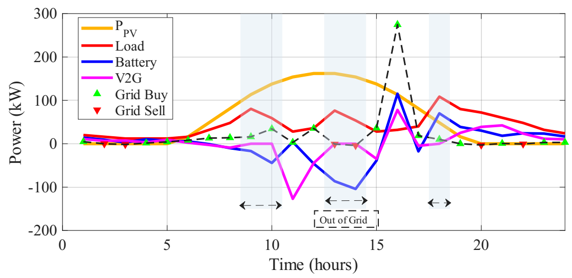

Figure 3. GA-optimized power flows

3.2. State-of-charge evolution

Figures 4 and 5 present SOC evolution for stationary battery and EV fleet. Figure 4 shows the battery cycles between 10-95%, while EV SOC maintains mobility readiness (>20%) and reaches target 80% by day end. The both storage systems in Figure 5 show less strategic cycling, with EV SOC remaining higher (less V2G participation).

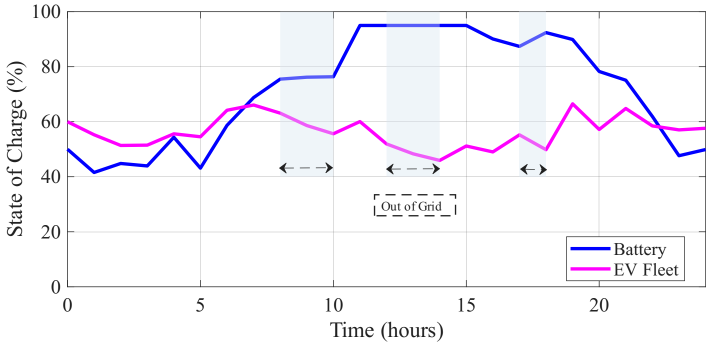

Figure 4. PSO-optimized SOC evolution

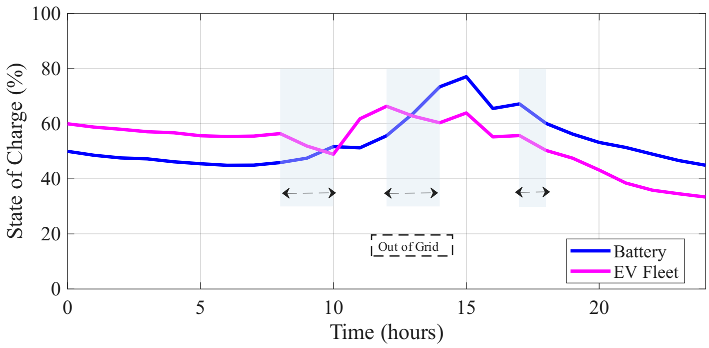

Figure 5. GA-optimized SOC evolution

3.3. Quantitative performance comparison

The results presented in Table 4 demonstrate the comparative performance of the hybrid PSO and GA approaches in terms of economic performance, energy utilization, and computational efficiency. Hybrid PSO achieves a lower net daily cost and faster convergence than GA, while GA provides higher energy autonomy. Overall, hybrid PSO offers better economic performance and computational efficiency, whereas GA provides greater energy autonomy.

3.4. Statistical validation

Table 5 presents results across 30 independent runs to assess robustness. Hybrid PSO achieves a lower net cost and higher energy sales than GA. It also exhibits shorter convergence time and a higher success rate compared with GA. These results confirm the superior robustness and consistency of hybrid PSO.

Table 4. Quantitative comparison: hybrid PSO vs GA

Metric	Hybrid PSO	GA	Metric	Hybrid PSO	GA
Net daily cost (€/day)	-279.14	100.07	Net grid balance (€/day)	-315.63	75.24
Energy sold (kWh/day)	2232.3	3.7	Energy autonomy (%)	28.0	67.9
Energy purchased (kWh/day)	739.2	329.0	Convergence time (s)	124	156
Revenue from sales (€/day)	486.11	1.30	Iterations to converge	87	142
Purchase cost (€/day)	170.49	76.54			

Table 5. Statistical results (30 runs, mean ± std)

Metric	Hybrid PSO	GA
Net cost (€/day)	-278.9 ± 8.4	101.2 ± 15.7
Energy sold (kWh/day)	2231.8 ± 45.2	4.1 ± 2.3
Convergence time (s)	125.3 ± 12.1	158.4 ± 18.6
Success rate (feasible solutions)	100%	96.7%

3.5. Sensitivity analysis

The sensitivity analysis shown as below: i) Impact of feed-in tariffs: Reducing feed-in tariffs by 20% decreases PSO revenue to 389 €/day but still yields net profit (-189 €/day). GA remains unprofitable (85 €/day) [20], [21]; ii) Impact of solar variability: Under ±15% solar irradiance uncertainty, PSO net cost ranges from -251 to -305 €/day, demonstrating robustness. GA remains positive (85-115 €/day) [22]; iii) System size scalability: Results for 10, 20, 40, and 80 households show consistent PSO advantage: cost reduction of 65-72% compared to GA across all scales [23], [24].

3.6. Discussion: why PSO outperforms GA

The superior performance of hybrid PSO can be attributed to three factors: i) memory-based search with personal and global best memories, ii) gradient local refinement via fmincon, and iii) effective constraint handling through velocity clamping and boundary projection [25].

4. CONCLUSION

This paper presented a systematic comparison between hybrid particle swarm optimization and genetic algorithm for V2G-enabled microgrid energy management applied to a 40-apartment residential system with 1000 m² of solar panels, 1 MWh of stationary battery storage, and 15 bidirectional electric vehicles. The simulation results demonstrate that hybrid PSO significantly outperforms GA across all economic and technical metrics. Specifically, the PSO-based approach achieves a net daily profit of 279 €, whereas GA incurs a net daily cost of 100 €, representing a performance gap of 379 € per day. This remarkable difference is primarily driven by PSO's ability to exploit profitable grid sales, generating 486 € per day in revenue compared to only 1.30 € per day for GA. Beyond economic performance, PSO also demonstrates superior computational efficiency, converging in 124 seconds (87 iterations) compared to 156 seconds (142 iterations) for GA, while maintaining 100% feasibility across 30 independent runs versus 96.7% for GA.

Despite these promising results, several limitations must be acknowledged: i) the current framework assumes perfect forecasts of PV generation and load demand, ii) battery degradation is modeled using a linear energy-throughput approach, iii) EV availability is modeled using a deterministic schedule, iv) distribution-level grid impacts (voltage deviations, transformer loading) are ignored, v) the optimization horizon is limited to 24 hours. Future work will address these limitations through stochastic optimization, nonlinear aging models, probabilistic mobility modeling, power flow integration, and multi-horizon planning. Ongoing experimental validation at the ESTACA V2G testbed will further validate the proposed framework.

ACKNOWLEDGMENTS

The authors would like to thank ESTACA LAB for providing the research facilities and the V2G testbed infrastructure used in this study.

FUNDING INFORMATION

Authors state no funding involved.

AUTHOR CONTRIBUTIONS STATEMENT

This journal uses the Contributor Roles Taxonomy (CRediT) to recognize individual author contributions, reduce authorship disputes, and facilitate collaboration.

Name of Author	C	M	So	Va	Fo	I	R	D	O	E	Vi	Su	P	Fu
Bilal Amghar	✓	✓	✓	✓	✓	✓		✓	✓	✓			✓	
Toufik Azib		✓				✓		✓	✓	✓	✓	✓		
Khelil Sidi Brahim	✓		✓	✓		✓			✓		✓		✓	

C	: **C**onceptualization	I	: **I**nvestigation	Vi	: **Vi**sualization
M	: **M**ethodology	R	: **R**esources	Su	: **Su**pervision
So	: **So**ftware	D	: **D**ata Curation	P	: **P**roject Administration
Va	: **Va**lidation	O	: Writing - **O**riginal Draft	Fu	: **Fu**nding Acquisition
Fo	: **Fo**rmal Analysis	E	: Writing - Review & **E**diting		

CONFLICT OF INTEREST STATEMENT

Authors state no conflict of interest.

DATA AVAILABILITY

The data that support the findings of this study are available from the corresponding author upon reasonable request.

REFERENCES

[1] International Energy Agency, "Renewables 2023 - analysis and forecast to 2028," *Paris*, vol. IEA Jan 20, p. 134, 2020, [Online]. Available: https://www.iea.org/reports/renewables-2023.

[2] S. Borenstein, "The private net benefits of residential solar PV: and who gets them," *Energy Institute at Haas Working Paper*, 2015.

[3] D. Dallinger, S. Gerda, and M. Wietschel, "Integration of intermittent renewable power supply using grid-connected vehicles – A 2030 case study for California and Germany," *Applied Energy*, vol. 104, pp. 666–682, Apr. 2013, doi: 10.1016/j.apenergy.2012.10.065.

[4] W. Kempton and J. Tomić, "Vehicle-to-grid power fundamentals: Calculating capacity and net revenue," *Journal of Power Sources*, vol. 144, no. 1, pp. 268–279, Jun. 2005, doi: 10.1016/j.jpowsour.2004.12.025.

[5] K. Clement-Nyns, E. Haesen, and J. Driesen, "The impact of charging plug-in hybrid electric vehicles on a residential distribution grid," *IEEE Transactions on Power Systems*, vol. 25, no. 1, pp. 371–380, Feb. 2010, doi: 10.1109/TPWRS.2009.2036481.

[6] E. S. Rigas, S. D. Ramchurn, and N. Bassiliades, "Managing electric vehicles in the smart grid using artificial intelligence: a survey," *IEEE Transactions on Intelligent Transportation Systems*, vol. 16, no. 4, pp. 1619–1635, 2015, doi: 10.1109/TITS.2014.2376873.

[7] M. R. Maghami, J. Pasupuleti, and J. Ekanayake, "Energy storage and demand response as hybrid mitigation technique for photovoltaic grid connection: challenges and future trends," *Journal of Energy Storage*, vol. 88, p. 111680, 2024, DOI: 10.1016/j.est.2024.111680.

[8] J. Sarda P. Patel, H. Patel, R. Vaghela, B. Brahma, A. K. Bhoi, and P. Barsocchi, "A review of the electric vehicle charging technology, impact on grid integration, policy consequences, challenges and future trends," *Energy Reports*, vol. 12, pp. 5671–5692, 2024, DOI: 10.1016/j.egyr.2024.11.047.

[9] M. H. Amrollahi and S. M. T. Bathaee, "Techno-economic optimization of hybrid photovoltaic/wind generation together with energy storage system in a stand-alone micro-grid subjected to demand response," *Applied Energy*, vol. 202, pp. 66–77, Sep. 2017, doi: 10.1016/j.apenergy.2017.05.116.

[10] J. Ihm, B. Amghar, S. Chun, and H. Park, "Optimum design of an electric vehicle charging station using a renewable power generation system in South Korea," *Sustainability*, vol. 15, no. 13, p. 9931, Jun. 2023, doi: 10.3390/su15139931.

[11] A. H. Gandomi, X. S. Yang, S. Talatahari, and A. H. Alavi, "Metaheuristic algorithms in modeling and optimization," *Metaheuristic Applications in Structures and Infrastructures*, pp. 1–24, 2013, doi: 10.1016/B978-0-12-398364-0.00001-2.

[12] R. T. Marler and J. S. Arora, "The weighted sum method for multi-objective optimization: new insights," *Structural and Multidisciplinary Optimization*, vol. 41, no. 6, pp. 853–862, Jun. 2010, doi: 10.1007/s00158-009-0460-7.

[13] J. Kennedy and R. Eberhart, "Particle swarm optimization," in *Proceedings of ICNN'95 - International Conference on Neural Networks*, IEEE, 1995, pp. 1942–1948. doi: 10.1109/ICNN.1995.488968.

[14] Y. Shi and R. Eberhart, "A modified particle swarm optimizer," in *1998 IEEE International Conference on Evolutionary Computation Proceedings. IEEE World Congress on Computational Intelligence (Cat. No.98TH8360)*, IEEE, 1998, pp. 69–73. doi: 10.1109/ICEC.1998.699146.

[15] A. R. Conn, N. I. M. Gould, and P. L. Toint, *Trust region methods*. Society for Industrial and Applied Mathematics, 2000. doi: 10.1137/1.9780898719857.

[16] J. Nocedal and S. J. Wright, *Numerical optimization*. in Springer Series in Operations Research and Financial Engineering. Springer New York, 2006. doi: 10.1007/978-0-387-40065-5.

[17] K. Pan, C.-D. Liang, and M. Lu, "Optimal scheduling of electric vehicle ordered charging and discharging based on improved gravitational search and particle swarm optimization algorithm," *International Journal of Electrical Power & Energy Systems*, vol. 157, p. 109766, Jun. 2024, doi: 10.1016/j.ijepes.2023.109766.

[18] D. T. Nguyen and L. B. Le, "Joint Optimization of Electric Vehicle and Home Energy Scheduling Considering User Comfort Preference," *IEEE Transactions on Smart Grid*, vol. 5, no. 1, pp. 188–199, Jan. 2014, doi: 10.1109/TSG.2013.2274521.

[19] M. M. Abdelaziz, A. Y. Abdelaziz, R. A. El-Sehiemy, and B. A.-E. Rashad, "Optimal scheduling of electric vehicle charging and discharging using two optimization paradigms," *Results in Engineering*, vol. 29, p. 108768, Mar. 2026, doi: 10.1016/j.rineng.2025.108768.

[20] H. Lund and W. Kempton, "Integration of renewable energy into the transport and electricity sectors through V2G," *Energy Policy*, vol. 36, no. 9, pp. 3578–3587, Sep. 2008, doi: 10.1016/j.enpol.2008.06.007.

[21] R. G. Allwyn, A. Al-Hinai, and V. Margaret, "A comprehensive review on energy management strategy of microgrids," *Energy Reports*, vol. 9, pp. 5565–5591, Dec. 2023, doi: 10.1016/j.egyr.2023.04.360.

[22] M. F. Zia, M. Benbouzid, E. Elbouchikhi, S. M. Muyeen, K. Techato, and J. M. Guerrero, "Microgrid Transactive Energy: Review, Architectures, Distributed Ledger Technologies, and Market Analysis," *IEEE Access*, vol. 8, pp. 19410–19432, 2020, doi: 10.1109/ACCESS.2020.2968402.

[23] S. Das, N. K. Yadav, and P. K. Jangilwar, "A multi-objective-based coordinated electric vehicle charging and discharging scheduling for grid support and cost efficiency," *Journal of Energy Storage*, vol. 139, p. 118789, Dec. 2025, doi: 10.1016/j.est.2025.118789.

[24] R. Benni, M. Sangeetha, M. S. Baroodwale, and D. Sarala, "Meta-heuristic algorithms for optimizing microgrid energy management: a comparative study," in *2024 Asian Conference on Intelligent Technologies (ACOIT)*, IEEE, Sep. 2024, pp. 1–8, doi: 10.1109/ACOIT62457.2024.10941318.

[25] C. Shang and F. You, "Data analytics and machine learning for smart process manufacturing: recent advances and perspectives in the big data era," *Engineering*, vol. 5, no. 6, pp. 1010–1016, Dec. 2019, doi: 10.1016/j.eng.2019.01.019.

BIOGRAPHIES OF AUTHORS

Bilal Amghar received his Ph.D. in Automatic Control, Electronics, and Electrical Engineering from ENSEA (University of Cergy, France) in 2013. He joined ESTACA in 2024 after six years at an ECAM group engineering school and five years at ESTP. He was responsible for several scientific projects including BCAPP (Qualified Business Check Application) and participated in academic and industrial research projects (Hydro+, Seinergy Lab, and SMART GRID). He has also supervised several Ph.D. theses on energy mix optimization (microgrid, smartgrid, and embedded energy). He is currently an associate professor and researcher in the field of energy (smart city, smart grids, and smart charging) at ESTACA Paris-Saclay Campus, France. He can be contacted at email: bilal.amghar@estaca.fr.

Toufik Azib received his Engineer degree in Electrotechnics (Electrical Control option) from Ferhat Abbas University Setif (UFAS), Algeria (2001-2006). He received his M.Sc. in Electrical and Electronic Engineering (power electronics and control track) from ENSEM - INPL Nancy, France (2006-2007). He earned his Ph.D. in Electrical Engineering from the University of Paris Sud XI (Laboratoire de Génie Electrique de Paris - LGEP) in 2010, with the dissertation titled ”Contribution à l’Etude d’Electro-générateur à Pile à Combustible. Conception d’Architectures et de Leurs Commandes” (with highest honors). He obtained his Habilitation à Diriger des Recherches (HDR) from Université Paris-Saclay (Doctoral School EOBE n°575) on the topic ”Contribution à la conception optimale des systèmes énergétiques embarqués: pré-dimensionnement et gestion d’énergie.” He is currently a professor at ESTACA Paris-Saclay and head of the ESTACA LAB energy group. His research focuses on power electronics, electric vehicle charging infrastructure, and smart grid integration. He can be contacted at email: toufik.azib@estaca.fr.

Khelil Sidi Brahim received his Ph.D. in Automatic Control from the University of Picardie Jules Verne, Amiens, France, in 2023. From 2022 to 2023, he was a Temporary Teaching and Research Attaché (ATER) at the LIS Laboratory and the Computer Science and Interactions Department of Aix-Marseille University. From 2023 to June 2024, he held a contract teaching position in the Industrial Engineering and Maintenance Department of IUT Chartres. Since July 2024, he has been an associate professor and researcher at ESTACA Paris-Saclay Campus. His current research focuses on the development of robust adaptive control mechanisms, trajectory tracking, autonomous vehicles, drones, and related applications. He can be contacted at email: khelil.sidibrahim@estaca.fr.